

# Lawrence Berkeley National Laboratory

## Lawrence Berkeley National Laboratory

### Title

Spectrally Resolved Magnetic Resonance Imaging of the Xenon Biosensor

### Permalink

<https://escholarship.org/uc/item/8b29986c>

### Authors

Hilty, Christian  
Lowery, Thomas  
Wemmer, David  
et al.

### Publication Date

2005-07-15

# Spectrally Resolved Magnetic Resonance Imaging of the Xenon Biosensor\*\*

*Christian Hilty, \* Thomas J. Lowery, David E. Wemmer, and Alexander Pines*

[\*] Dr. C. Hilty, Prof. A. Pines  
Lawrence Berkeley National Laboratory, Materials Sciences Division, and University of California Berkeley, Department of Chemistry, Berkeley CA 94720, USA  
Fax: +1 (510) 486 5744  
E-mail: hilty@berkeley.edu

T. Lowery, Prof. D. Wemmer  
Lawrence Berkeley National Laboratory, Physical Biosciences Division, and University of California Berkeley, Department of Chemistry, Berkeley CA 94720, USA

[\*\*] This work was supported by the Director, Office of Science, Office of Basic Energy Sciences, Materials Sciences and Engineering Division, of the U.S. Department of Energy under Contract No. DE-AC03-76SF00098. C.H. acknowledges support from the Schweizerischer Nationalfonds through a post-doctoral fellowship. T.L. acknowledges support from the University of California Biotechnology Research and Education Program for a training grant.

Due to its ability to non-invasively record images, as well as elucidate molecular structure, nuclear magnetic resonance is the method of choice for applications as widespread as chemical analysis and medical diagnostics. Its detection threshold is, however, limited by the small polarization of nuclear spins in even the highest available magnetic fields. This limitation can, under certain circumstances, be alleviated by using hyper-polarized substances.<sup>[1]</sup> Xenon biosensors make use of the sensitivity gain of hyperpolarized xenon to provide magnetic resonance detection capability for a specific low-concentration target.<sup>[2-4]</sup> They consist of a cryptophane cage,<sup>[5]</sup> which binds one xenon atom, and which has been connected via a linker to a targeting moiety such as a ligand or antibody. Recent work has shown the possibility of using the xenon biosensor to detect small amounts of a substance in a heterogeneous environment by NMR.<sup>[6]</sup> Here, we demonstrate that magnetic resonance (MR) provides the capability to obtain spectrally and spatially resolved images of the distribution of

immobilized biosensor, opening the possibility for using the xenon biosensor for targeted imaging.

A continuous flow of water saturated with hyperpolarized xenon was supplied by a specifically designed apparatus (see experimental section) to ~250  $\mu\text{l}$  immobilized avidin-agarose beads packed in a glass tube assembly between two frits (see Figure 2a). The xenon biosensor was attached to the agarose beads through the affinity of its biotin tag to immobilized avidin (binding affinity of  $10^{-15} \text{ M}^{-1}$ ). From biochemical characterization, it was estimated that a biosensor concentration of 82  $\mu\text{M}$  was thus achieved in the resin. The biosensor construct that was used is shown in Figure 1, with its xenon-binding cryptophane cage to the right and its biotin tag at the bottom of the drawing.

In a  $^{129}\text{Xe}$  NMR spectrum of this sample (Figure 1), the peak at 65.4 ppm, with a linewidth of 300 Hz, corresponds to xenon in biosensor. The downfield peaks at 193.6 and 192.5 ppm are from dissolved xenon in agarose beads and water, respectively,<sup>[6]</sup> and the 0 ppm peak is from xenon gas. The xenon resonance from the immobilized biosensor is broadened when compared to that for solution-free biosensor (~20 Hz),<sup>[2,7]</sup> presumably due to motional hindrance of the cage.

A spectrally resolved image of the biosensor distribution in this sample was acquired using phase encoded MR imaging (Figure 2). For comparison, Figure 2a shows a photograph of the sample with flowing xenon-saturated water. Drawn to scale with this photograph is the xenon image that has spatial resolution along the z-axis (Figure 2b). It is readily apparent that different regions of the sample give rise to the peaks with different chemical shift. Image intensity at the dissolved chemical shift (~193 ppm) extends over the entire sample space, while the peak at the chemical shift of xenon in the biosensor (65.4 ppm) occurs only in the actual volume of the beads. To the right of the image, a short section of xenon gas (0 ppm) is visible, which corresponds to the region in the sample where gas bubbles appear in the photograph (Figure 2a). This outgassing is due to a pressure gradient over the column of

beads. The spectral dimension in Figure 2b is processed with a sine bell window selecting only the first part of the free induction decay (FID), where biosensor signal is present. As a consequence, in this image the peak of dissolved xenon is not resolved into its water and bead components. When applying an exponential window function that extends over the entire FID, the splitting of this peak becomes readily observable (Figure 2c). Here, the extent of the bead volume can be deduced from the peak at 193.6 ppm, closely corresponding to the extent of the biosensor peak.

These experiments show that MR imaging of selectively targeted xenon biosensor can be accomplished with good sensitivity. Using hyperpolarized xenon, the distribution of a micromolar range concentration of avidin could be imaged in this heterogeneous sample. In comparison, direct detection of bead-bound avidin with proton NMR would be very difficult or impossible due to low concentration, broad linewidth and spectral crowding.

Imaging at the lower NMR coil filling factors required for most in situ samples will demand significant sensitivity improvements. More than a factor of ten in signal could easily be gained by using a xenon polarizer optimized for continuous flow applications,<sup>[8]</sup> giving a polarization of ~50% instead of ~3%. Another factor of fifteen could be gained by using a biosensor that does not suffer broadening of the xenon line when immobilized. Further sensitivity could be gained by designing sensor constructs that contain more than one xenon binding cage per analyte, and by using of isotopically enriched xenon. These improvements would boost the sensitivity of xenon biosensor imaging by a factor of at least 1,000, which extrapolates to a detection threshold of ~100 nM in a small NMR coil optimized for the biosensor-bound sample volume, or to a detection limit of ~100  $\mu$ M in a sample of the present size in an overall volume of several liters.

From these results, one may extrapolate the potential usefulness of a xenon biosensor construct that is targeted to markers on cell surfaces. In vivo imaging with free hyperpolarized xenon has already been demonstrated.<sup>[9,10]</sup> In combination with specific targeting, for example

to tumor cells, this could lead to a new tool for medical applications such as the diagnosis of cancer. For detection of low target concentrations in opaque tissue, the xenon biosensor would offer advantages over other methods. In contrast to using hyperpolarized small molecules,<sup>[11]</sup> the biosensor could be injected well in advance to hyperpolarized xenon introduction and signal acquisition, allowing adequate time for target binding without compromising xenon polarization. As seen in Figure 2b, xenon in the biosensor is easily distinguished from bulk xenon through its difference of chemical shift. A xenon biosensor image therefore is an image with near-zero background, and should afford much higher detection fidelity than a contrast agent such as gadolinium that merely modulates the proton signal already present in the entire volume.<sup>[12]</sup> The large chemical shift bandwidth of cage-encapsulated xenon makes possible the use of the xenon biosensor for multiplexed analysis, where a number of different biosensors with unique xenon chemical shifts bind to different targets.<sup>[2,4]</sup> Our results here indicate that the possibility of multiplexed biomolecular analysis can be extended to imaging to allow for multiple, target-selective images to be acquired simultaneously (see Figure 2), which would greatly enhance the specificity and fidelity of diagnosis.

## Experimental Section

An apparatus (Figure 3) was designed to provide a continuous stream of liquid saturated with hyperpolarized xenon. Water flowed from the liquid supply (1000 ml) to the bubbling cell (5 ml), where it was saturated with hyperpolarized xenon ( $4.4 \text{ mM}\cdot\text{atm}^{-1}$ )<sup>[1,6]</sup> (Amersham Health, Durham, NC), then through the sample to the “liquid out” port. Hyperpolarized xenon gas mixture (1% Xe at natural isotope abundance, polarized to ~3%, mixed with 10% N<sub>2</sub>, 89% He; Airgas, Radnor, PA) was supplied with a pressure of 6 atm to the “gas in” port, and flowed through the bubbling cell to the “gas out” port. The gas also pressurized the liquid supply, so that gravity was sufficient to flow liquid to the bubbling cell. Both the liquid refill and the sample flow rates were controlled with needle valves and measured with rotameters. To ensure that the bubbling cell did not empty during an experiment, the refill rate was set 50% higher than the flow rate through the sample. The excess water exited the bubbling cell together with the gas and was collected in the overflow tank. The bubbling intensity was controlled via the gas flow rate (0.7 standard liters per minute), which was adjusted at the “gas out” port. System pressure was monitored at the inlet to the overflow tank.

For the present experiments, the sample of immobilized-avidin, 6% cross-linked, agarose beads (Pierce Biotechnology) with xenon biosensor was designed to fit within the coil of a 10 mm NMR probe (Varian, Palo Alto, CA), which had a sensitive region of 1.8 cm along the z-axis. The probe was inserted together with a gradient coil assembly into a vertical bore superconducting NMR magnet (7 T). Using the described apparatus, the sample was efficiently perfused by xenon saturated water, which refreshed itself completely every 6 s when using a liquid flow rate of 10 ml/min. The bubbling cell was located immediately above the sample.

Spectrally resolved MR images were acquired using phase encoding for spatial dimensions and chemical shift resolved acquisition.<sup>[13]</sup> The pulse sequence was thus  $p_{90} - \tau_{\text{grad}} - p_{180} - \tau_{\text{acq}}$ .  $p_{90} = 14 \mu\text{s}$  and  $p_{180} = 28 \mu\text{s}$  stand for rf pulses with the indicated flip angle,

phase encoding gradients were applied during  $\tau_{\text{grad}} = 200 \mu\text{s}$ , and the spectral dimension was acquired as an echo during  $\tau_{\text{acq}} = 100 \text{ ms}$ . The phases of the  $90^\circ$  pulse and the receiver were cycled as  $\{x, -x\}$ . A delay of 6 s between transients was used.

Keywords: biosensors · NMR spectroscopy · imaging agents · xenon · cage compounds

- [1] M. G. Mortuza, S. Anala, G. E. Pavlovskaya, T. J. Dieken, T. Meersmann, *J. Chem. Phys.* **2003**, *118*, 1581-1584.
- [2] M. M. Spence, E. J. Ruiz, S. M. Rubin, T. J. Lowery, N. Winssinger, P. G. Schultz, D. E. Wemmer, A. Pines, *J. Am. Chem. Soc.* **2004**, *126*, 15287-15294.
- [3] T. J. Lowery, S. M. Rubin, E. J. Ruiz, M. M. Spence, N. Winssinger, P. G. Schultz, A. Pines, D. E. Wemmer, *Magn. Reson. Imaging* **2003**, *21*, 1235-1239.
- [4] M. M. Spence, S. M. Rubin, I. E. Dimitrov, E. J. Ruiz, D. E. Wemmer, A. Pines, S. Q. Yao, F. Tian, P. G. Schultz, *Proc. Natl. Acad. Sci. USA* **2001**, *98*, 10654-10657.
- [5] A. Collet, *Tetrahedron* **1987**, *43*, 5725-5759.
- [6] S. I. Han, S. Garcia, T. J. Lowery, E. J. Ruiz, J. A. Seeley, L. Chavez, D. S. King, D. E. Wemmer, A. Pines, *Anal. Chem.* **2005**, *77*, 4008-4012.
- [7] T. J. Lowery, S. Garcia, L. Chavez, E. J. Ruiz, T. Wu, T. Brotin, J.-P. Dutasta, D. S. King, P. G. Schultz, A. Pines, D. E. Wemmer, *Submitted* **2005**.
- [8] K. Knagge, J. Prange, D. Raftery, *Chem. Phys. Lett.* **2004**, *397*, 11-16.
- [9] M. S. Albert, G. D. Cates, B. Driehuys, W. Happer, B. Saam, C. S. Springer, A. Wishnia, *Nature* **1994**, *370*, 199-201.
- [10] B. M. Goodson, Y. Q. Song, R. E. Taylor, V. D. Schepkin, K. M. Brennan, G. C. Chingas, T. F. Budinger, G. Navon, A. Pines, *Proc. Natl. Acad. Sci. USA* **1997**, *94*, 14725-14729.
- [11] K. Golman, J. H. Ardenaer-Larsen, J. S. Petersson, S. Mansson, I. Leunbach, *Proc. Natl. Acad. Sci. USA* **2003**, *100*, 10435-10439.
- [12] M. L. Wood, P. A. Hardy, *JMRI-J. Magn. Reson. Im.* **1993**, *3*, 149-156.
- [13] P. T. Callaghan, *Principles of Nuclear Magnetic Resonance Microscopy*, Oxford University Press, New York, **1991**.



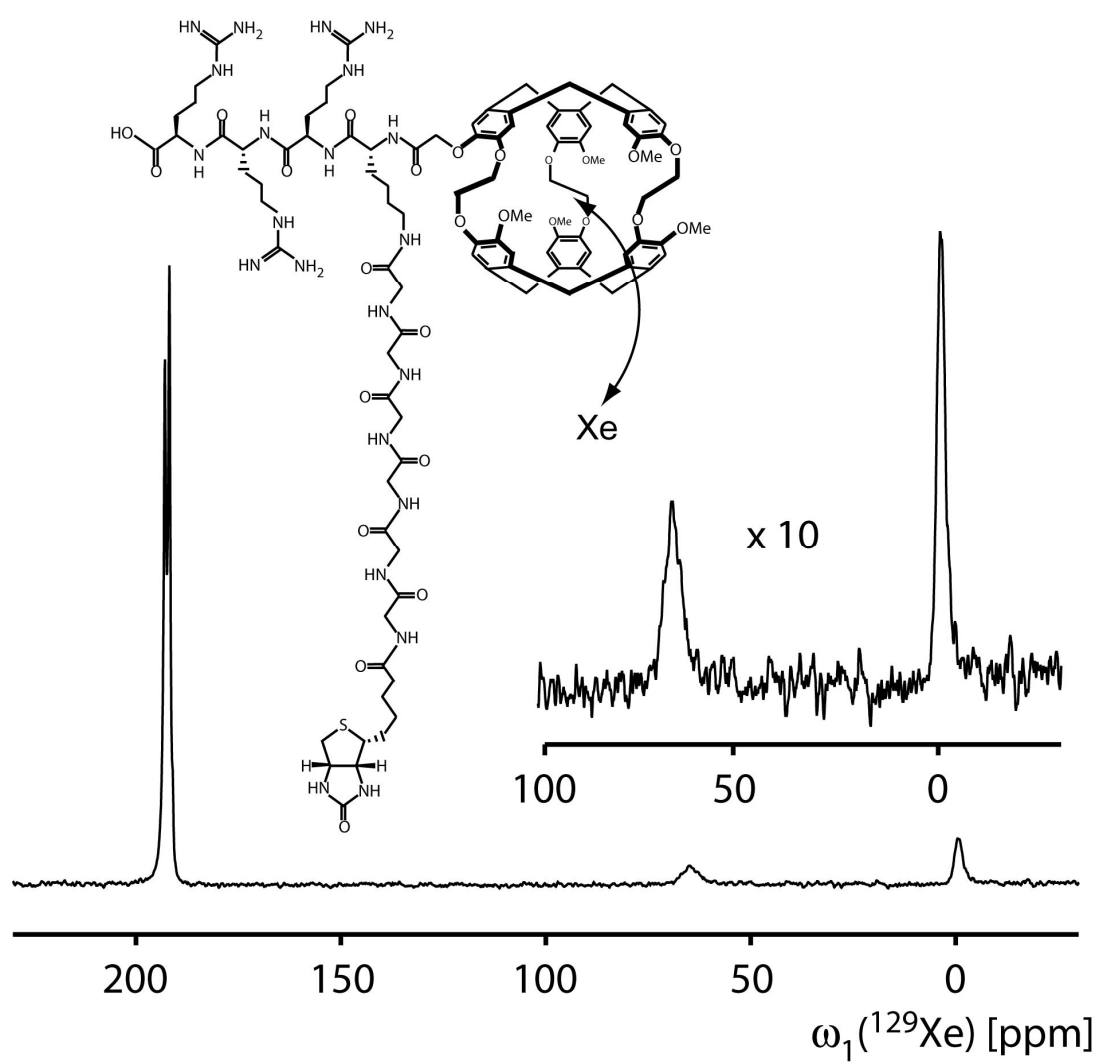


**Figure 1.** Chemical structure of the functionalized xenon biosensor;<sup>[2,6]</sup> NMR spectrum of xenon biosensor bound to avidin containing agarose beads.

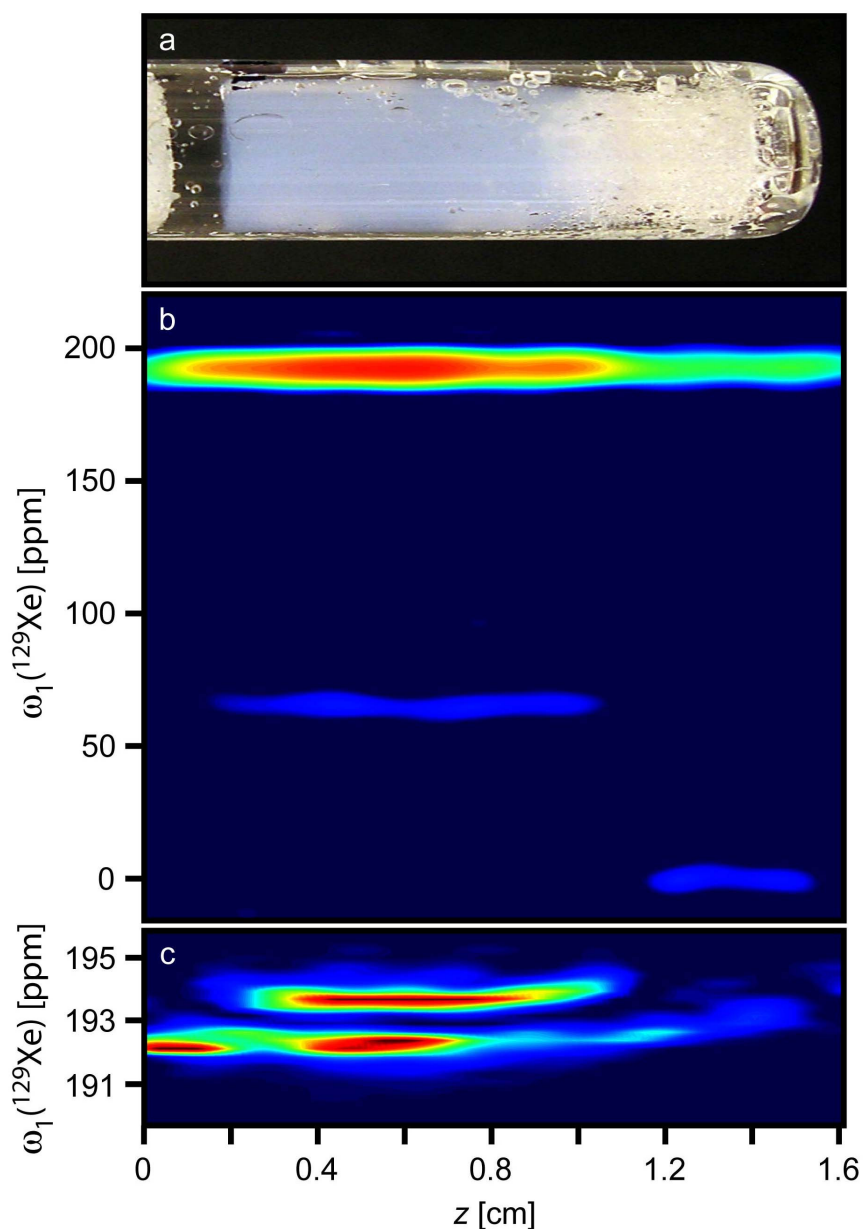


**Figure 2.** a) Photograph of the agarose bead sample used for the imaging experiments. The direction of liquid flow is from left to right, through the column of beads, out the frit and around the outside of the inner concentric tube. b) Spectrally resolved MR image of immobilized xenon biosensor. The image dimension (horizontal) is shown to scale with the photograph in a. The image was taken in 135 min, using a field of view along the  $z$ -dimension of 2 cm and a resolution of 1.2 mm. c) Image of solution peak in b, processed to show splitting between xenon in bead and xenon in water.

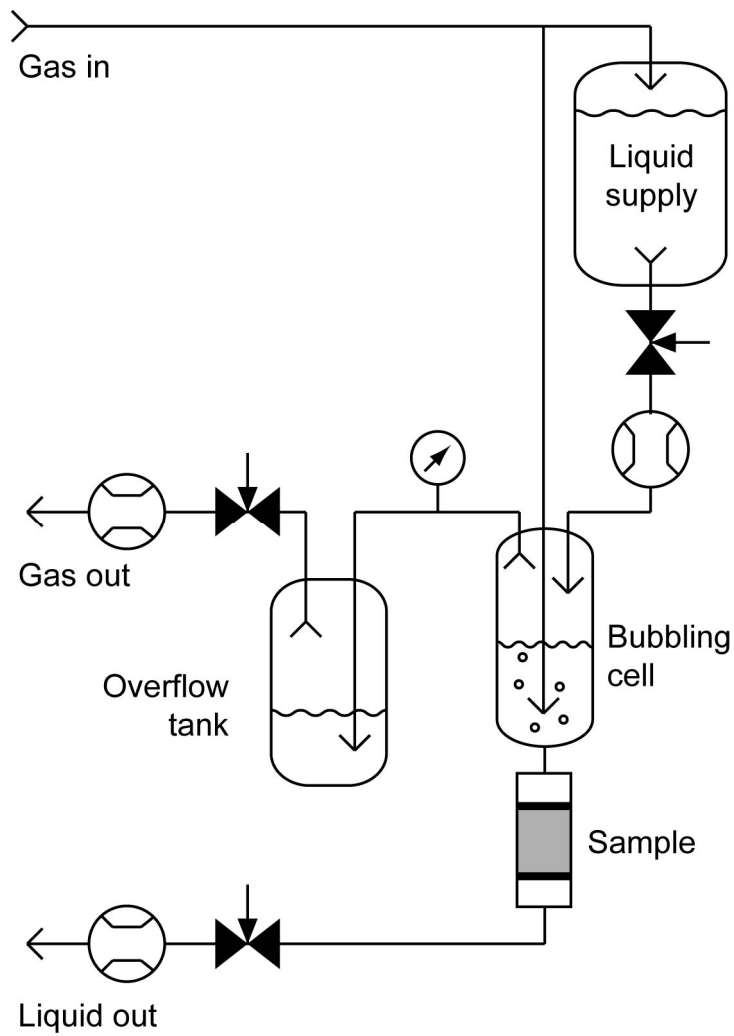


**Figure 3.** Instrumentation for MR imaging with xenon saturated liquids.